Applied Materials Today 18 (2020) 100530

Contents lists available at ScienceDirect

Applied Materials Today

journal homepage: www.elsevier.com/locate/apmt

Electrochemically driven multi-material 3D-printing

Adriano Ambrosi[a], Richard D. Webster[a], Martin Pumera[b,c,d,e,*]

[a] Division of Chemistry & Biological Chemistry, School of Physical and Mathematical Sciences, Nanyang Technological University, 637371, Singapore
[b] Future Energy and Innovation Lab, Central European Institute of Technology, Brno University of Technology, Purkyňova 656/123, Brno, CZ-616 00, Czech Republic
[c] Department of Chemical and Biomolecular Engineering, Yonsei University, 50 Yonsei-ro, Seodaemun-gu, Seoul 03722, Republic of Korea
[d] Department of Medical Research, China Medical University Hospital, China Medical University, No. 91 Hsueh-Shih Road, Taichung, Taiwan
[e] Center for Advanced Functional Nanorobots, Dept. of Inorganic Chemistry, Faculty of Technology, University of Chemistry and Technology Prague, 16200, Czech Republic

ARTICLE INFO

Article history:
Received 20 September 2019
Received in revised form 2 December 2019
Accepted 4 December 2019

Keywords:
3D-printing
Additive manufacturing
Electrochemistry
Metal printing
Conductive polymer printing
Multimaterial 3D-printing

ABSTRACT

Major efforts for the advancement of additive manufacturing are lately focused on the development of multi-material 3D-printing (mMat-3DP) methods which can enable the fabrication of complete devices in a single printing process combining materials with different properties (structural, functional, conductive, etc.). Printing conductive (metal and non-metal) materials with low-energy-consuming and economical methods is of particular interest since it would facilitate the production of electrodes, catalytic surfaces and electronic circuitry in general for countless applications. In order to contribute to the future vision of mMat-3DP, we wish to show here an economical method to selectively deposit different conductive materials (metal and conductive polymer) by means of electrochemical driving forces. A custom-made electrochemical liquid dispenser with embedded electrodes is used to electrodeposit selectively a metal (Cu), a conductive polymer (polyaniline), or a combination of the two, with both precursors present simultaneously and conveniently in the common electrolytic bath. Combining the 3D-patterning ability of a desktop 3D-printer with a concurrent control of the electrochemical process, selective deposition is demonstrated over a conductive graphite foil used as the cathode. Printing and electrochemical parameters have been optimized using scanning electron microscopy and energy dispersive X-ray spectroscopy to characterize the printed structures. The electrochemical 3D-printing method, being inherently low-cost, scalable and compatible with electrode fabrication methods shall find a broad scope of applications.

© 2019 Published by Elsevier Ltd.

1. Introduction

Multi-material 3D-printing, particularly for metals, generally employed for the fabrication of electronic devices [1], is currently possible using extrusion deposition with metallic nanoparticle-based inks [2–5]. While a large variety of ink formulations are possible, there are important drawbacks with the use of this technique: i) it is difficult to have similar rheological properties for different inks to enable common printing parameters; ii) the printed metallic structures possess inferiors conductive and mechanical properties than those obtained with full metals, demanding therefore post-printing thermal treatments and iii) optimization of the ink composition is tedious and time-consuming [6]. Better mechanical and conductive properties can be achieved using powder-based metal printing which however i) requires expensive machines with high energy consuming lasers and vacuum chambers and ii) can only print a single metal at a time [7–9]. A different approach to print metallic structures is based on electrochemical deposition [10,11]. One approach consists on the use of microelectrode probes immersed in a bath of the metal salt solution and in the vicinity of a conductive substrate. When the microelectrode approaches the substrate, which acts as the cathode, the focused electric field produces localized reduction of the metal onto the substrate [12–14]. Another approach is based on the use of micropipettes that contain the metal salt solution and the anode electrode. When the pipette tip approaches the conductive substrate (cathode), the formation of a liquid meniscus is established and controlled confined electrodeposition of the metal can occur onto the substrate applying the appropriate potential difference [15]. The use of piezo-driven positioning devices and micro/nanopipette dispensers, metallic micro and nanoscale structures have been obtained. Seol et al. showed how the variation of amplitude and duration of the potential applied can produce

* Corresponding author at: Center for Advanced Functional Nanorobots, Dept. of Inorganic Chemistry, Faculty of Technology, University of Chemistry and Technology Prague, 16200, Czech Republic
E-mail address: pumera.research@gmail.com (M. Pumera).

https://doi.org/10.1016/j.apmt.2019.100530
2352-9407/© 2019 Published by Elsevier Ltd.

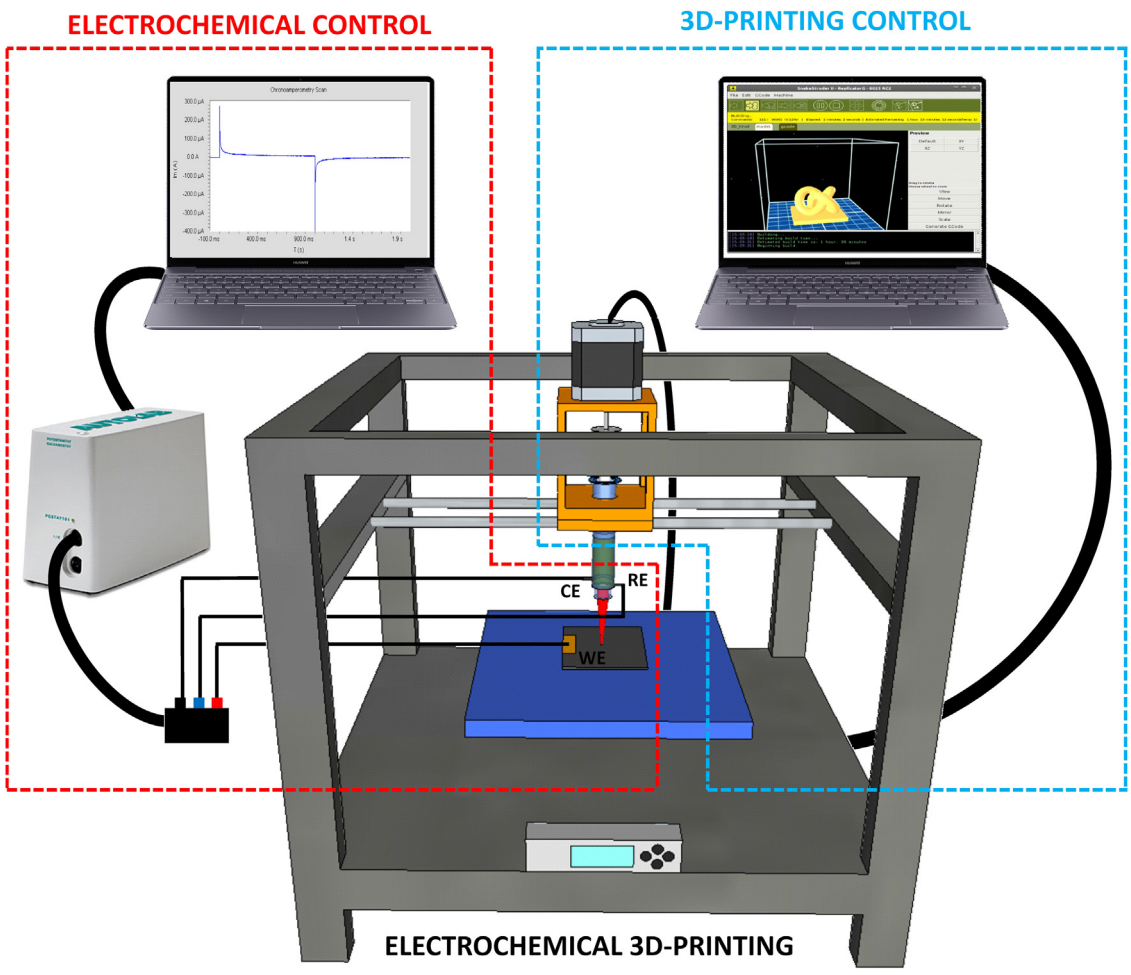

Fig. 1. Schematic of the electrochemical 3D-printing system.

either rod or tubular copper microstructures [16]. Lin et al. recently developed a microprinting device able to create extraordinary high-density, ultrahigh aspect ratio 3D metallic structures with even nanoscale precision [17]. In another work an AFM cantilever probe with a square aperture at the tip of about 0.25 μm^2 was used to produce sub-micrometer copper structures [18]. In addition to metals, microprinting of conductive polymer (polyaniline) structures, were also demonstrated by means of a dual barrel micropipette used in a scanning electrochemical microscopy system [19]. These methods represent valid alternatives to conventional ink-based and laser-based printing technologies but are also limited to micro and nanoscale applications, can be hardly scaled-up to produce macrostructures and still require expensive piezo-driven positioning systems. A more economical metal printing technology is highly needed, particularly to enable large-scale fabrication possibly with multiple metals. Chen et al. recently proposed an electrochemical method based on a commercial desktop 3D-printer, a syringe-like liquid dispenser carrying a nozzle plastic tip of about 0.4 mm opening. Authors demonstrated meniscus confined electrodeposition of copper structures investigating the effect of potential applied between the anode copper rod inside the syringe and the copper substrate used as the cathode. Large potentials up to 6 V were applied to produce millimetre scale structures with lateral movement speed of 0.4 mm/s [20]. The same authors more recently improved the system achieving larger deposition rates by employing an electrospun nanofibre nib inside the nozzle to create a more stable meniscus while ensuring fast transfer of metal ions from the bulk solution within the syringe and the tip. Also multimetal printing was demonstrated with two syringe dispensers, one for copper and one for nickel, to fabricate thermally responsive actuators [21].

Here we propose a simple and economical large-scale meniscus-confined electrochemical printing method to fabricate multimaterial structures employing a single extrusion dispenser. A modified commercial desktop 3D-printer is used for the spatially controlled movement of the syringe which allocates inside a pseudo-reference Ag/AgCl wire electrode and a Pt strip counter electrode. We show how by simply selecting the appropriate deposition potential to the conductive substrate used as the working electrode, a precise control over the material to be deposited can be obtained. This concept is demonstrated using copper metal ions and aniline precursors which are conveniently introduced together inside the dispenser. Once the meniscus is formed between the nozzle and the substrate which connects all the electrodes, the selection of a cathodic or anodic potential to the substrate can produce the selective deposition of metal copper or polyaniline (PANI) conductive polymer, respectively. An electrochemical analyser connected to the electrodes is used to set the desired potential and also to monitor the meniscus formation and the deposition process by measuring the current signal generated. Optimization of the deposition conditions was carried out with the support of electron microscopy (SEM) and EDX element analysis characterization tools. Finally a simple proof-of-concept multimaterial circuit fabrication is proposed combining the two materials into a single object.

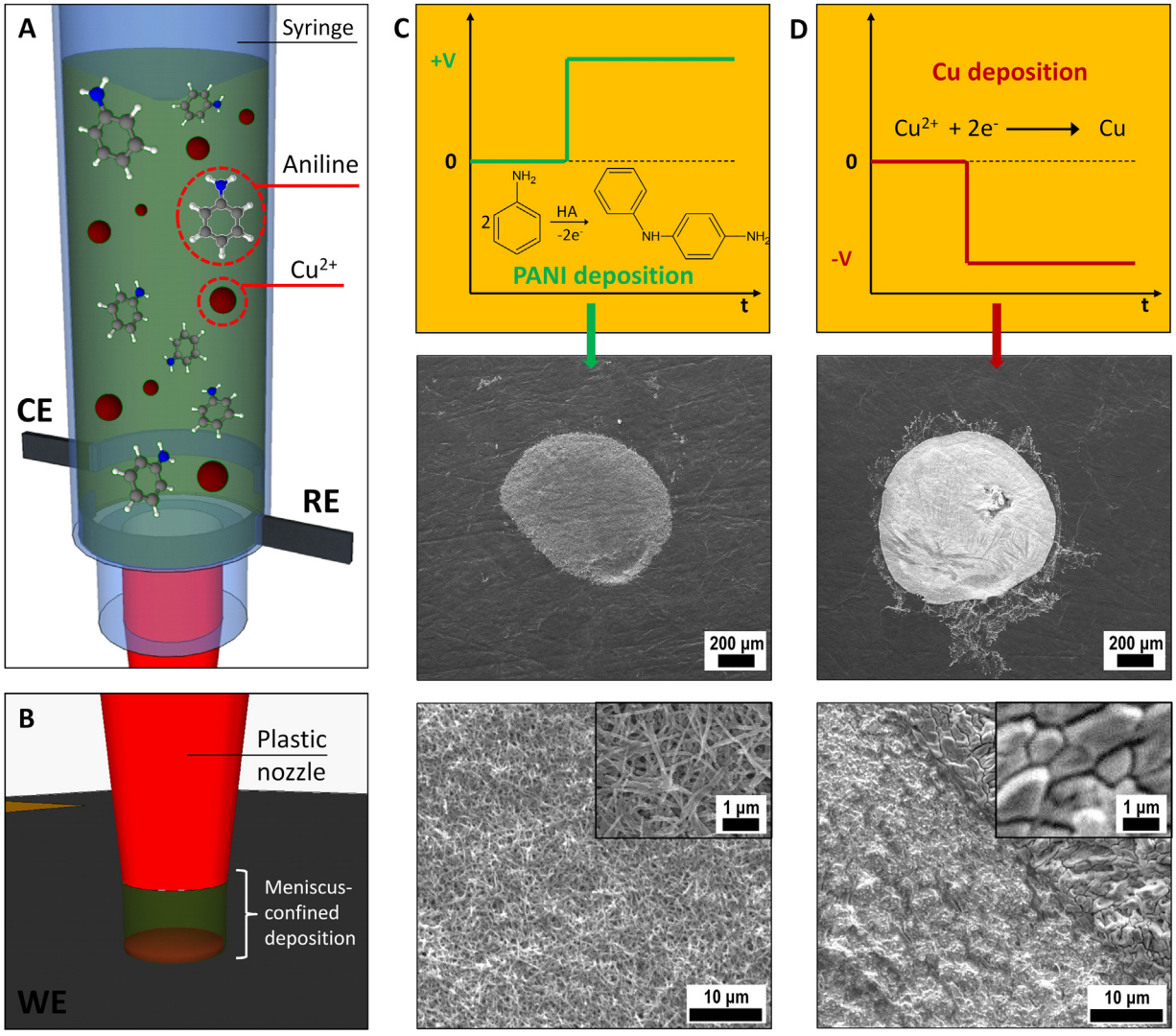

Fig. 2. A) Enlarged view of the syringe dispenser with highlighted the compounds present in the deposition solution, and also the position of the reference electrode (RE, Ag/AgCl) and counter electrode (CE, Pt) with external connections. B) Enlarged view of the meniscus formation when solution comes into contact with the substrate working electrode (WE, graphite foil). C) Application of anodic potential (+V) facilitates the polymerization of aniline to polyaniline (PANI) with its typical filamentous structure as seen in SEM images below. D) Application of cathodic potential (-V) triggers the deposition of copper metal which possess a typical brick-like conformation as seen in SEM images below.

2. Materials and methods

2.1. Materials

$CuSO_4 \cdot 6H_2O$, aniline hydrochloride, perchloric acid were purchased from Sigma–Aldrich, Singapore.

2.2. Apparatus

A commercially available FDM 3D-printer (Flashforge Creator Pro) was modified replacing the hot end extruder with a syringe holder employing the filament stepper motor to control the syringe plunger movement. Simplify3D software was employed to slice the printing design and input the printing job and also to manually control the printer movements during optimization studies. A modified 10 mL disposable plastic syringe was used as the material dispenser carrying a plastic tip with opening diameter of 0.25 or 0.6 mm as nozzle. A Pt strip and an Ag/AgCl wire were inserted inside the syringe as counter and reference electrodes, respectively. Two small holes carefully sealed were used to connect the electrodes to the electrochemical analyser without interfering with the syringe plunger movement. Autolab PGSTAT101 electrochemical analyzer (Methrom Autolab B. V., The Netherlands) connected to a personal computer and controlled by NOVA software Version 1.8 (Methrom Autolab B. V.) was used to control the electrochemical processes monitoring the current responses while applying the fixed printing potentials. Pictures of the actual printing system are provided in Fig. S1 of Supporting Information. A three-electrode electrochemical system was created using a graphite foil as working electrode which also acted as printing platform onto which the materials are printed. Scanning Electron Microscopy (SEM) images and EDX element mapping were obtained by using Jeol 7600 F SEM (Jeol, Japan) operating at 5 kV.

2.3. Procedures

Solution for printing consisted of 1 M $CuSO_4$, 0.2 M aniline in 1 M $HClO_4$ electrolyte. $HClO_4$ was chosen because while being compatible with the copper reduction process, it facilitates the formation of more compact PANI films compared to H_2SO_4 which produces more porous structures [22]. The syringe dispenser was filled with the printing solution and located onto the holder where a care-

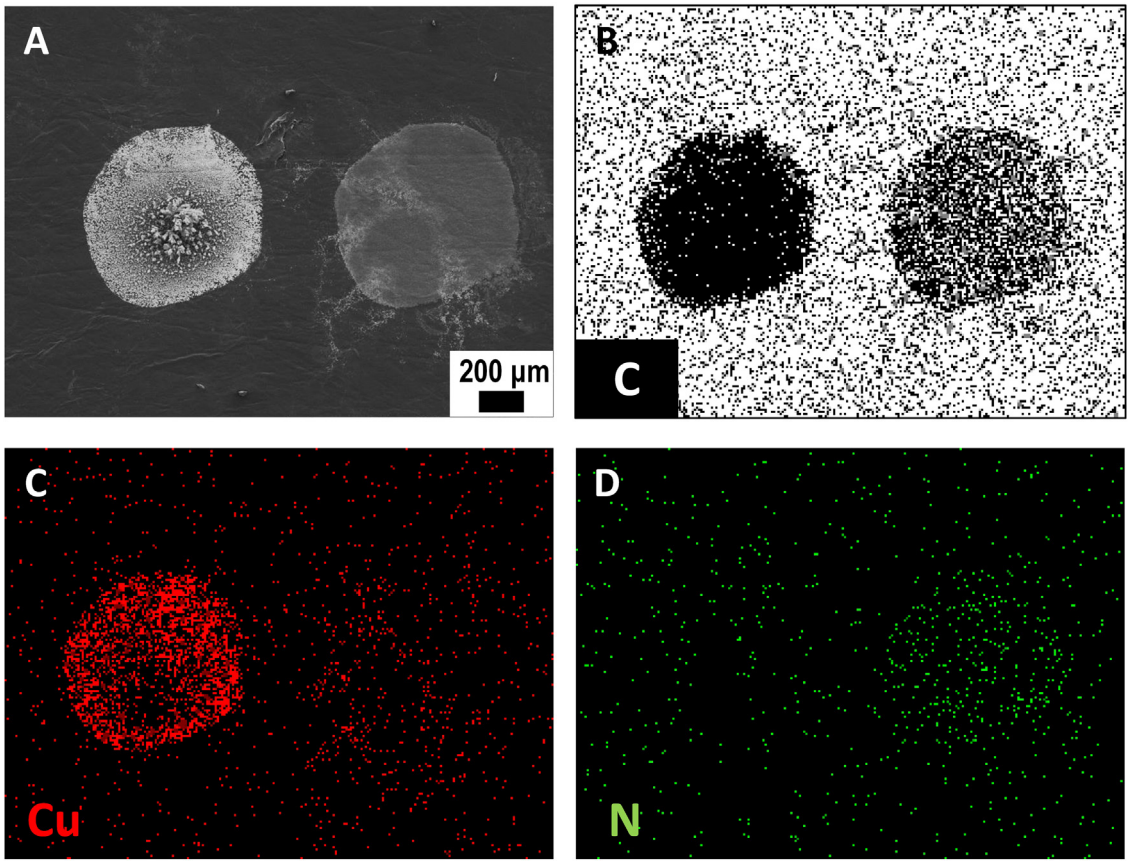

Fig. 3. A) SEM image of Cu (left) and PANI (right) structures printed applying cathodic (−0.6 V) and anodic (+0.9 V), respectively, for a period of 300 s. EDX element mapping analysis showing the presence of B) carbon (white), C) copper (red) and D) nitrogen (green).

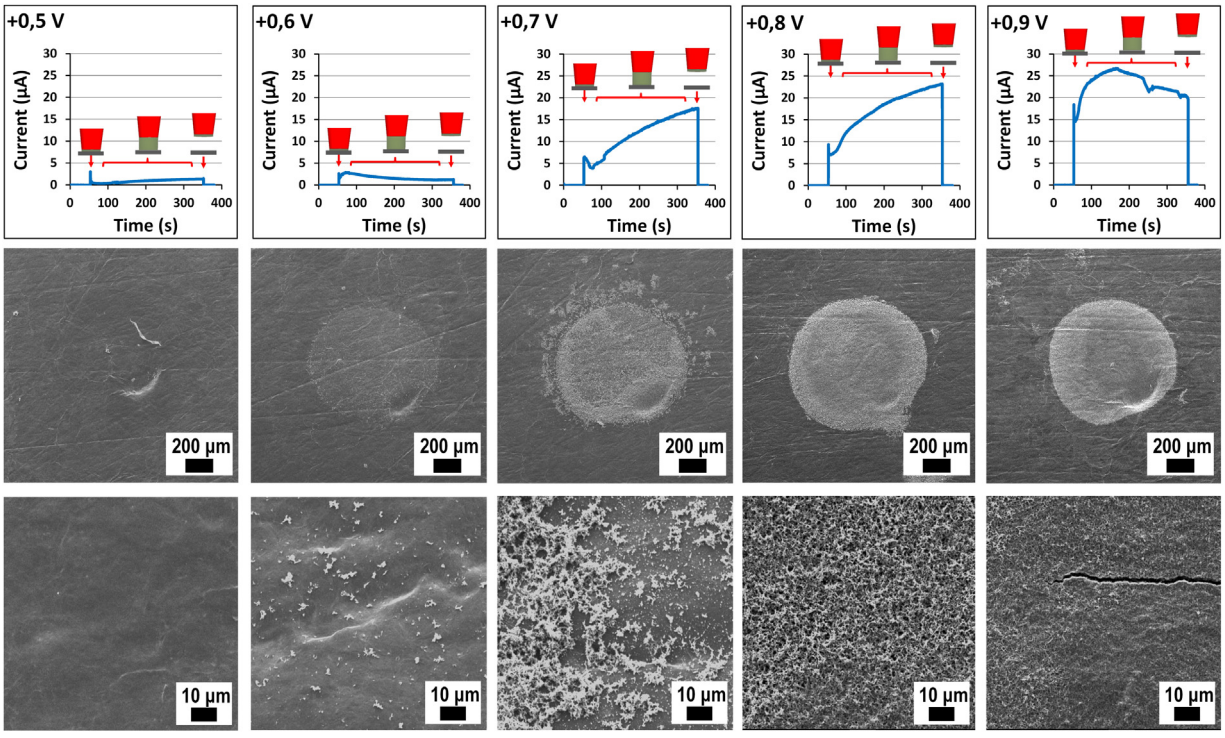

Fig. 4. Anodic deposition of PANI at different potentials with corresponding current measurement (top), SEM image at low magnification (middle) and SEM image at higher magnification (bottom). Inset inside the chronoamperogram (top) describes, in correspondence to the measured current, the moment when the nozzle touches the substrate, when the meniscus is formed and when the nozzle withdraws at the end of the process. Deposition duration, 300 s.

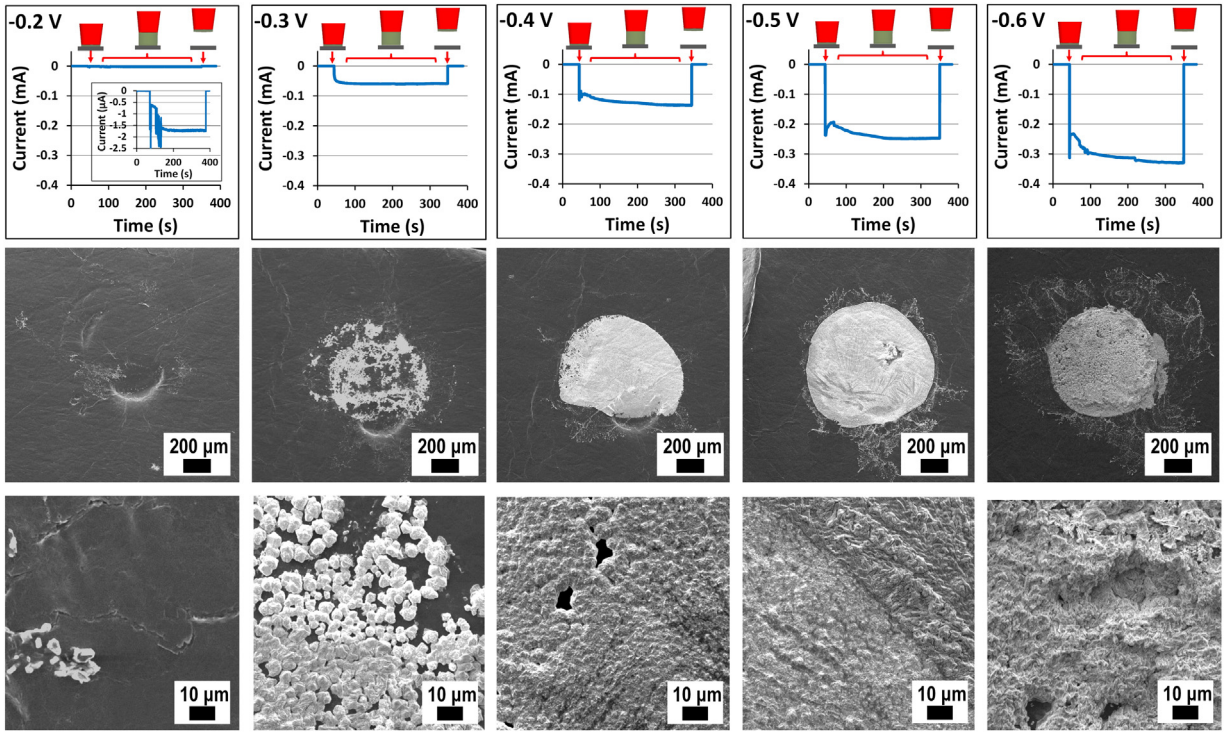

Fig. 5. Cathodic deposition of copper at different potentials with corresponding current measurement (top), SEM image at low magnification (middle) and SEM image at higher magnification (bottom). Inset inside the chronoamperogram (top) describes, in correspondence to the measured current, the moment when the nozzle touches the substrate, when the meniscus is formed and when the nozzle withdraws at the end of the process. Deposition duration, 300 s.

ful connection between the plunger and the motor was ensured. NOVA software was used to control the electrochemical process. In particular the application of a fixed printing potential (anodic or cathodic) was set between the working electrode (graphite foil) and the reference electrode (Ag/AgCl wire) while monitoring the current response. Such response is useful to control the formation of the meniscus. A slow and control approach of the nozzle to the stage is manually done using the Simplify3D software control jug. When the nozzle tip touches the stage a current signal is recorded which is proportional to the potential applied. Then a withdraw movement of 0.2 mm (the stage is actually lowered) produces a meniscus cylinder of 0.6 mm diameter (nozzle opening size) and 0.2 mm high (separation between stage and nozzle). In this way a reproducible meniscus is always generated during all the printing processes. This was set as the optimal meniscus volume. Once the meniscus is created the printing process can proceed for the period planned. The current signal is continuously monitored providing not only information on the efficiency of the process but also as indicator of any interruption due to evaporation of the solution, nozzle detachment, etc. PANI deposition is obtained applying a fixed potential of +0.9 V (vs Ag/AgCl) while copper deposition is obtained applying −0.6 V potential. Multimaterial printing can be set by alternating the cathodic and the anodic potentials for fixed period of times within the same printing procedure.

3. Results and discussion

In order to develop a low-cost printing system, we modified a commercial fused deposition modelling (FDM) printer replacing the hot end extruder with a syringe liquid dispenser. Using a custom-made 3D-printed holder the syringe plunger and the x-y-z movements are computer controlled with the 3D-printer software. The syringe dispenser is modified introducing inside a reference Ag/AgCl wire pseudo-reference electrode and a Pt strip counter electrode both connected externally to the electrochemical analyser but without interfering with the plunger movement. Electrochemical control is obtained using an electrochemical analyser connected to a personal computer and controlled by electrochemical workstation software. Plastic tips connected to the syringe can be used as deposition nozzles and which come with different opening sizes ranging from 0.2 mm to 1 mm diameter. The working electrode chose in this work consisted of a graphite foil which is fixed onto the printing stage and connected to the analyser through a copper tape. Fig. 1 describes the schematic of the electrochemical 3D-printing setup with highlighted the electrochemical control unit (red) and the 3D-printing control unit (x-y-z movement, blue). Photos of the actual system are provided in Supporting information file as Fig. S1. More details on the modified syringe can be found in the experimental section.

An enlarged visualization of the modified syringe can be seen in Fig. 2A in which both the reference (RE) and counter (CE) electrodes are illustrated together with the solution used for the multimaterial printing consisting of the metallic ionic specie (Cu^{2+}) and the conductive polymer precursor (aniline). The electrochemical control is enabled by the formation of a micro-electrochemical cell when the liquid inside the syringe comes into contact with the conductive substrate creating a well-defined meniscus whose size depends on the nozzle opening and the distance between the nozzle and the substrate. The electrodeposition (meniscus-confined electrodeposition) can thus be controlled with the application of a well-defined potential to the working electrode (WE) against the reference and counter electrodes which share the same solution. Deposition occurring within the meniscus volume is also spatially controlled through the 3D-printing motors which move the syringe onto the substrate (Fig. 2B).

In this work we demonstrate that the application of anodic or cathodic potentials applied to the substrate can dictate what material deposits without any contamination. Precisely, the application of an anodic potential (vs Ag/AgCl) can drive the formation of aniline radicals which then polymerize onto the substrate forming

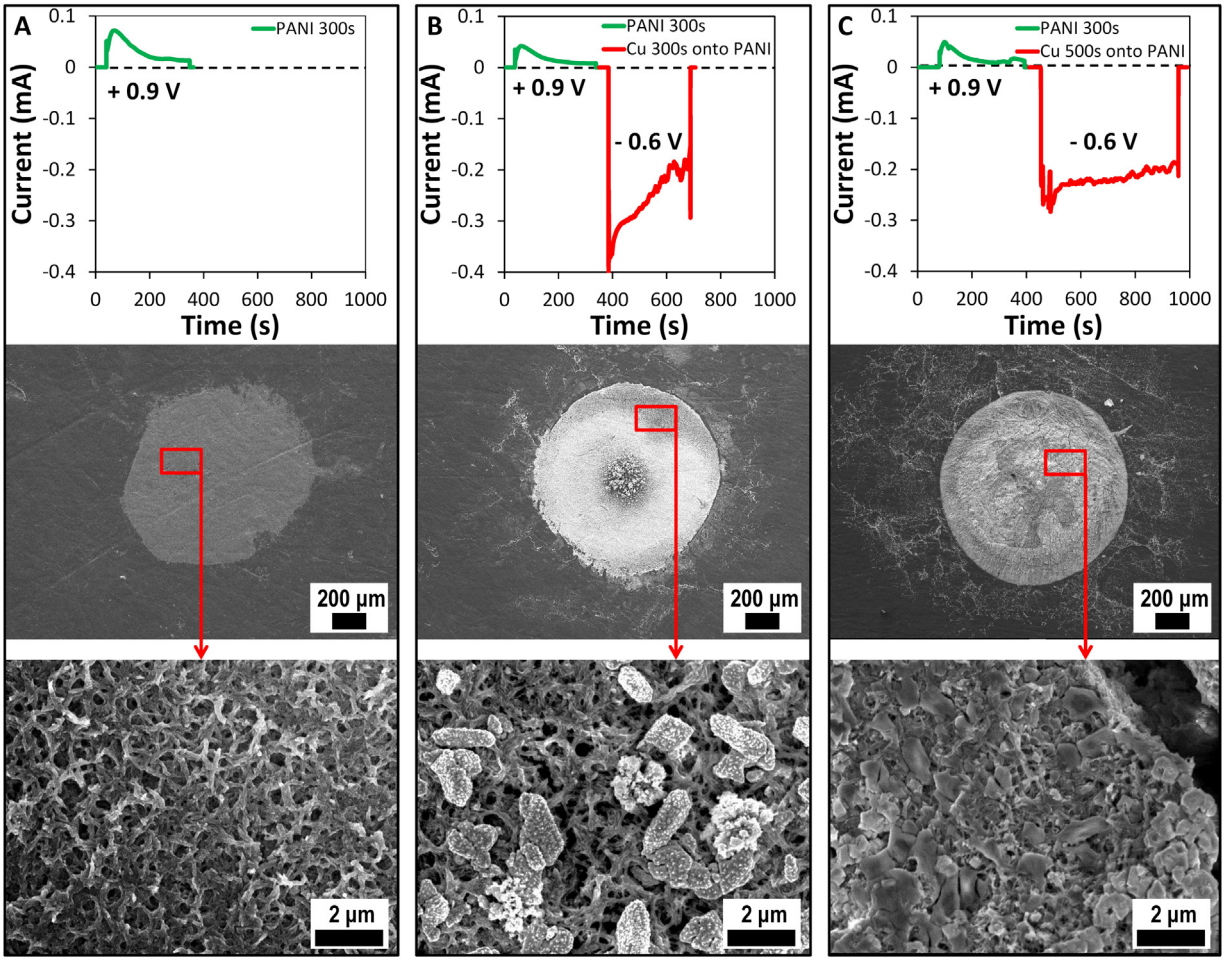

Fig. 6. A) Chronoamperogram (top) and corresponding SEM images at low magnification (middle) and high magnification (bottom) for PANI deposited at +0.9 V for 300 s. B) Chronoamperogram (top) and corresponding SEM images at low magnification (middle) and high magnification (bottom) for PANI deposited at +0.9 V for 300 s followed by copper deposition at −0.6 V for 300 s. C) Chronoamperogram (top) and corresponding SEM images at low magnification (middle) and high magnification (bottom) for PANI deposited at +0.9 V for 300 s followed by copper deposition for 500 s.

solid polyaniline (PANI) conductive polymer [22] with the typical filamentous/porous structure as evidenced in Fig. 2C. Cu^{2+} ions remain in solution since no electrochemical process occurs at this potential. On the other end, a cathodic potential facilitates the deposition of copper with the electroreduction of the Cu^{2+} ions. Aniline molecules also present in the same solution are not activated at this potential and therefore do not interfere with or contaminate the formation of the metallic copper structures which present typical brick-type features (Fig. 2D).

In order to demonstrate the selectivity of the printing procedure two disc-shaped structures were printed next to each other using cathodic (left) and anodic (right) potentials for the deposition of copper and PANI, respectively. Fig. 3 shows the SEM images of the structures with the corresponding elemental analysis mapping obtained by EDX spectroscopy. It can be seen how the left structure consists solely of Cu while the right structure has nitrogen and carbon as the predominant elements characteristic with PANI polymer. In addition it should be pointed out that the spatial separation between the structures is easily and precisely controlled through the 3D-printer software with a resolution of 0.1 mm which corresponds to the stepper motors minimal movement. The abundant carbon element outside the printed structures comes from the graphite foil substrate.

We investigated separately the anodic and cathodic processes in order to understand the influence of the potential applied to the material depositions. As for the anodic process, different potentials between +0.5 V and +0.9 V are applied while monitoring the current generated during the deposition of the PANI polymer. This allows also a precise control over the formation of the meniscus since the current signal can be used as feedback when the nozzle approaches the cathode surface, touches it, creates the meniscus and finally withdraws (Fig. 4). We observed the material deposited by SEM after the application of each potential for a period of 300 s. As it can be seen a potential of +0.5 V is not sufficient to drive the polymer formation, while PANI deposits can be seen starting from +0.6 V potential applied. It is evident that a more and more compact and thicker polymer deposition is achieved by increasing the deposition potential achieving highly compact deposits when the potential of +0.9 V is applied. Further increase in anodic potential is known to deteriorate the PANI polymer [22,23] and therefore we opted to use +0.9 V as the optimal. The current recorded at each potential provides also good indication of the efficiency of the process reaching the highest values applying +0.8 V and +0.9 V. Using +0.9 V as the potential to be applied for the deposition we also investigated different deposition times between 100 s and 500 s. Homogeneous PANI deposits are readily formed already after 100 s although with a more porous polymer structure. A compact structure is formed at 300 s and 500 s (see Fig. S2 of Supporting Information).

Similarly, we investigated the cathodic process by applying different potentials between −0.2 V and −0.6 V for a constant period of 300 s. Fig. 5 summarizes the current recorded during the deposition process for each applied potential with the corresponding SEM

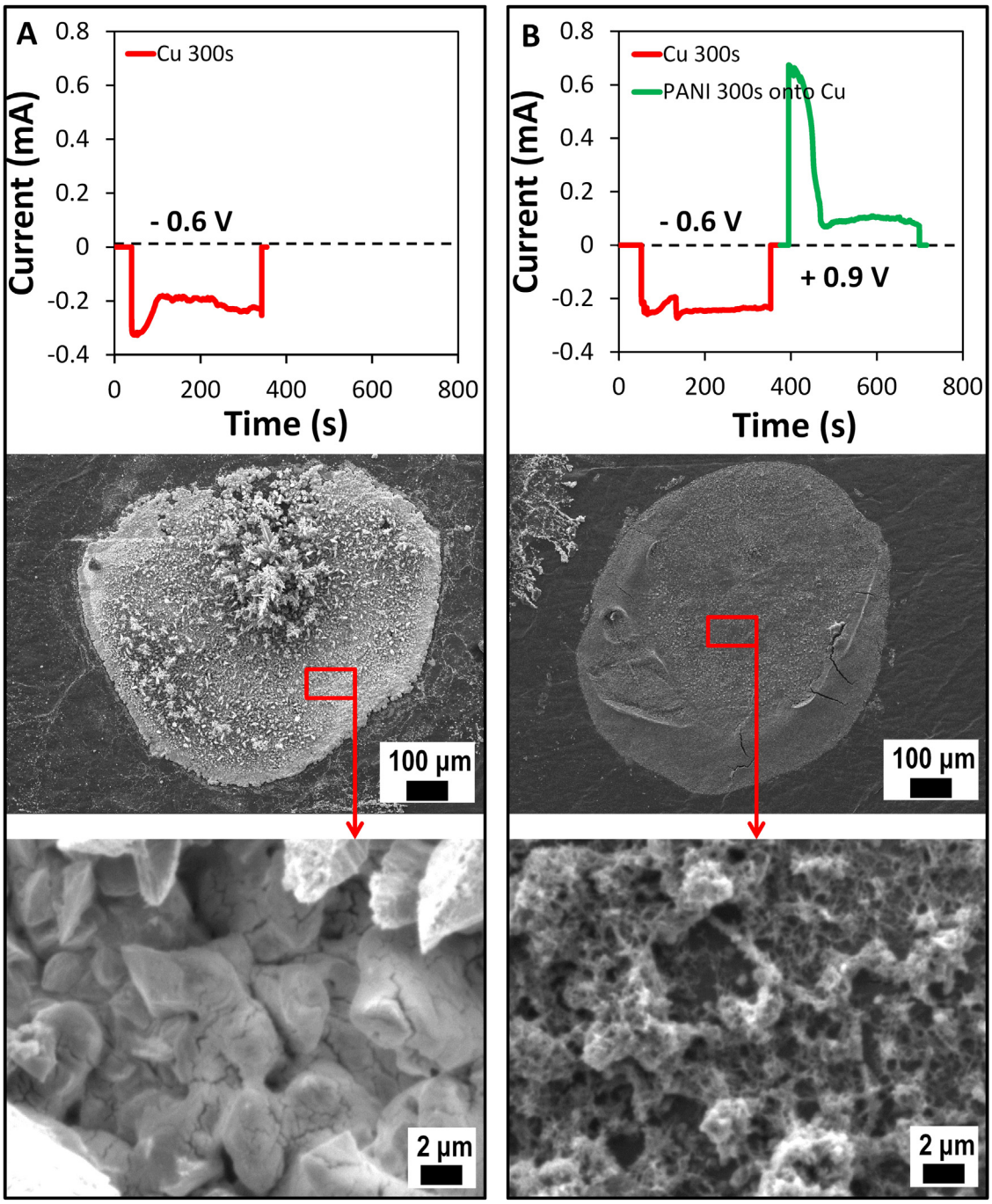

Fig. 7. A) Chronoamperogram (top) and corresponding SEM images at low magnification (middle) and high magnification (bottom) for copper deposited at −0.6 V for 300 s. B) Chronoamperogram (top) and corresponding SEM images at low magnification (middle) and high magnification (bottom) for copper deposited at −0.6 V for 300 s followed by PANI deposition at +0.9 V for 300 s.

images of the material formed. It can be seen that little to no deposition is obtained by applying −0.2 V which is insufficient to drive the reduction of the copper ions to metal copper. Deposition can be seen when applying the potential of −0.3 V although with poor efficiency. More negative potentials produced efficient depositions with −0.6 V being the potential generating fast, homogeneous and compact Cu deposits. Potential more negative than −0.6 V can drive the reduction of water together with copper deposition with thus the undesired formation of H_2 bubbles. These bubbles interfere with the formation of a stable meniscus as well as with the formation of a compact deposit (see Fig. S3 of Supporting Information). We thus selected −0.6 V as the optimal for the copper deposition. Again monitoring the current produced during the deposition can be used as feedback to achieve a controlled formation of the meniscus.

Multimaterial printing is then demonstrated by applying sequentially different deposition potentials so that two different materials can be deposited one on top of each other. It is again important to highlight that this multi-material printing is obtained by simply selecting the optimized potential, using the same extruder and without changing material precursors. We firstly tested the possibility to print sequentially PANI followed by a Cu disc which therefore seats onto the PANI polymer. To obtain this, an anodic potential of +0.9 V is firstly applied for 300 s fol-

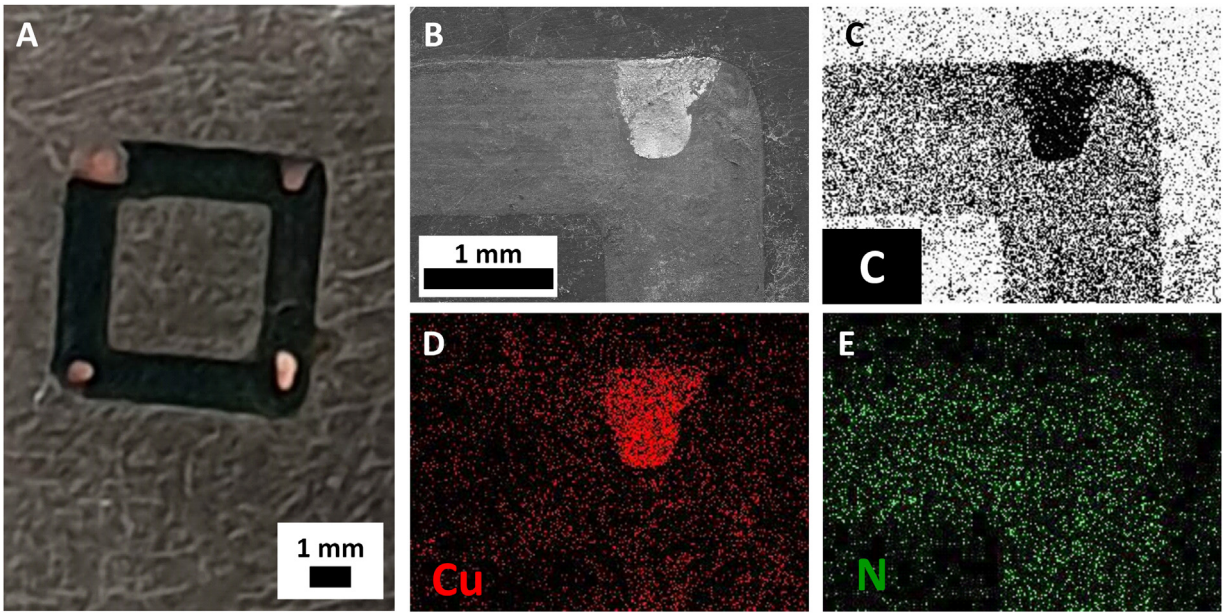

Fig. 8. A) Picture of the completed PANI based square circuit (5 × 5 mm) with copper connections deposited at the four corners. B) SEM image of one corner of the structure. Corresponding element mapping for C) carbon, D) copper and E) nitrogen are also shown.

lowed, with only few seconds interval, by a cathodic potential of −0.6 V. Fig. 6 shows the current recorded during the depositions with the corresponding SEM images of the materials deposited. It can be seen in Fig. 6B that copper deposits are formed on top of the PANI polymer although leaving exposed some sections of the polymer underneath. This is clearly visible in the image at higher magnification. In order to obtain a full coverage of the PANI polymer by the copper deposit, a longer deposition time of 500 s was used (Fig. 6C). Clearly using longer deposition time a more compact copper film is obtained and fully covering the polymer. Fig. 6A shows the deposition of solely the PANI polymer so to facilitate a visual comparison of the material structures once deposited. It is evident that the selection of the material to be deposited can be easily tuned by simply selecting the deposition potential.

Inverting the sequence by firstly starting with the cathodic potential and followed by the anodic one, PANI polymer can be deposited onto the copper (Fig. 7). In this case, however, it should be noticed that a partial dissolution of the copper occurs during the initial PANI formation since the anodic potential is sufficient to re-oxidize the copper metal to Cu^{2+} ions. This is evident monitoring the current during the PANI deposition. It can be noticed in Fig. 7B that during the initial PANI deposition a large current signal is recorded, which is due to the electrochemical oxidation of copper. PANI film is then obtained covering fully the copper underneath. Fig. 7A shows the current signal recorded for the deposition of copper as well as the microscopy images of the structure for comparison purposes. The high magnification images clearly evidence once again the different structural features of copper and PANI.

A tentative 3D-printed multi-material circuit fabrication is finally attempted as proof-of-concept. A simple square-shaped 5 × 5 mm structure is firstly designed using CAD software; this is then translated to instructions to the 3D-printer to move the extruder onto the graphite cathode in agreement with the design to deposit PANI. The anodic potential of +0.9 V is applied for 1 h to allow good multi-layer deposition. A speed of movement of 0.3 mm/s was selected for this task as the optimal to enable good PANI deposition while preserving a stable meniscus during the movement for the entire process. This corresponds to about 54 multiple passes of the extruder obtaining a well visible thick PANI structure (Fig. 8A). Once completed the PANI deposition, four small copper structures were set to deposit at the corner of the PANI structure. For these, a deposition time of 15 min each was set to guarantee homogeneous and visible deposition. Fig. 8A shows the picture of the completed printed structure. SEM image (Fig. 8B) highlights one corner of the structure with the copper deposited onto the PANI structure. The corresponding EDX element mapping images are shown in Fig. 8C–E to confirm the presence of carbon, copper and nitrogen, respectively. It can be seen that copper structures were successfully deposited at the four corners of the PANI square circuit as dictated by the design. EDX analysis confirms the selectivity of the deposition for each material achieved by the selection of the electrochemical potential. Higher magnification SEM images of the multi-material structure are provided in Figs. S4 and S5 of supporting information highlighting the Cu and PANI structures, respectively.

4. Conclusions

We demonstrated here how electrochemistry can be adopted to selectively drive multimaterial printing by simply selecting the appropriate deposition potential. A single printing extruder/dispenser containing both copper ions and aniline can be used to selectively print metal copper and PANI structures onto a conductive substrate. Deposition is achieved through the formation of a stable meniscus between the substrate and the extruder nozzle (tip). The selection of an anodic potential can drive the formation of PANI conductive polymer via the formation of the aniline radicals. Copper metal printing, instead, is achieved by selecting a cathodic potential which can reduce the copper ions to copper metal onto the substrate with no reaction occurring for the aniline sharing the solution. Monitoring the current generated during the deposition for each potential applied could also provide precious information on the formation of the meniscus facilitating reproducible operations. Current feedback can in fact be used to detect when the nozzle touches the substrate surface, the formation of a stable meniscus and also detect signal interruptions and/or nozzle withdrawn. SEM and EDX analysis were used to confirm selective deposition and microscopic structural features of the materials printed. A tentative proof-of-concept 3D-printed multi-material circuit is finally provided combining PANI structure and copper connections into a

single printing process. This new electrochemical multimaterial 3D printing technique is low-cost, versatile, scalable and it has broad applicability to many areas of applications, from flexible sensors to neuroscience.

Contributions

A.A. designed and performed all experiments and analysis. R. D. W. and M.P. designed and supervised the work.

Declaration of Competing Interest

The authors declare no competing financial interest.

Acknowledgments

This work was supported by the project Advanced Functional Nanorobots (reg. No. CZ.02.1.01/0.0/0.0/15_003/0000444 financed by the EFRR). R.W. acknowledges A*Star grant (No. SERC A1783c0005), Singapore.

Appendix A. Supplementary data

Supplementary material related to this article can be found, in the online version, at doi:https://doi.org/10.1016/j.apmt.2019.100530.

References

[1] A. Ambrosi, M. Pumera, 3D-printing technologies for electrochemical applications, Chem. Soc. Rev. 45 (2016) 2740–2755.
[2] B.Y. Ahn, E.B. Duoss, M.J. Motala, X. Guo, S.-I. Park, Y. Xiong, J. Yoon, R.G. Nuzzo, J.A. Rogers, J.A. Lewis, Omnidirectional printing of flexible, stretchable, and spanning silver microelectrodes, Science 323 (2009) 1590–1593.
[3] P. Galliker, J. Schneider, H. Eghlidi, S. Kress, V. Sandoghdar, D. Poulikakos, Direct printing of nanostructures by electrostatic autofocussing of ink nanodroplets, Nat. Commun. 3 (2012) 890.
[4] A. Elkoro, L. Soler, J. Llorca, I. Casanova, 3D printed microstructured Au/TiO2 catalyst for hydrogen photoproduction, Appl. Mater. Today 16 (2019) 265–272.
[5] C. Cano-Raya, Z.Z. Denchev, S.F. Cruz, J.C. Viana, Chemistry of solid metal-based inks and pastes for printed electronics – a review, Appl. Mater. Today 15 (2019) 416–430.
[6] J.O. Hardin, T.J. Ober, A.D. Valentine, J.A. Lewis, Microfluidic Printheads for Multimaterial 3D Printing of Viscoelastic Inks, Adv. Mater. 27 (2015) 3279–3284.
[7] J.-Y. Lee, J. An, C.K. Chua, Fundamentals and applications of 3D printing for novel materials, Appl. Mater. Today 7 (2017) 120–133.
[8] A. Ambrosi, J.G.S. Moo, M. Pumera, Helical 3D-Printed metal electrodes as custom-shaped 3D platform for electrochemical devices, Adv. Funct. Mater. 26 (2016) 698–703.
[9] Z.H. Liu, D.Q. Zhang, S.L. Sing, C.K. Chua, L.E. Loh, Interfacial characterization of SLM parts in multi-material processing: metallurgical diffusion between 316L stainless steel and C18400 copper alloy, Mater. Charact. 94 (2014) 116–125.
[10] W. Schindler, P. Hugelmann, M. Hugelmann, F.X. Kärtner, Localized electrochemical nucleation and growth of low-dimensional metal structures, J. Electroanal. Chem. 522 (2002) 49–57.
[11] J.D. Madden, I.W. Hunter, Three-dimensional microfabrication by localized electrochemical deposition, J. Microelectromechanical Syst. 5 (1996) 24–32.
[12] R.A. Said, Localized electro-deposition (LED): the march toward process development, Nanotechnology 15 (2004) S649–S659.
[13] E.M. El-Giar, R.A. Said, G.E. Bridges, D.J. Thomson, Localized electrochemical deposition of copper microstructures, J. Electrochem. Soc. 147 (2000) 586–591.
[14] S.-K. Seol, A.-R. Pyun, Y. Hwu, G. Margaritondo, J.-H. Je, Localized electrochemical deposition of copper monitored using real-time X-ray microradiography, Adv. Funct. Mater. 15 (2005) 934–937.
[15] J. Hu, M.-F. Yu, Meniscus-confined three-dimensional electrodeposition for direct writing of wire bonds, Science 329 (2010) 313–316.
[16] S.K. Seol, D. Kim, S. Lee, J.H. Kim, W.S. Chang, J.T. Kim, Electrodeposition-based 3D printing of metallic microarchitectures with controlled internal structures, Small 11 (2015) 3896–3902.
[17] Y.-P. Lin, Y. Zhang, M.-F. Yu, Parallel process 3D metal microprinting, Adv. Mater. Technol. 4 (2019), 1800393.
[18] L. Hirt, S. Ihle, Z. Pan, L. Dorwling-Carter, A. Reiser, J.M. Wheeler, R. Spolenak, J. Vörös, T. Zambelli, Template-Free 3D microprinting of metals using a force-controlled nanopipette for layer-by-layer electrodeposition, Adv. Mater. 28 (2016) 2311–2315.
[19] K. McKelvey, M.A. O'Connell, P.R. Unwin, Meniscus confined fabrication of multidimensional conducting polymer nanostructures with scanning electrochemical cell microscopy (SECCM), Chem. Commun. 49 (2013) 2986–2988.
[20] X. Chen, X. Liu, P. Childs, N. Brandon, B. Wu, A low cost desktop electrochemical metal 3D printer, Adv. Mater. Technol. 2 (2017), 1700148.
[21] X. Chen, X. Liu, M. Ouyang, J. Chen, O. Taiwo, Y. Xia, P.R.N. Childs, N.P. Brandon, B. Wu, Multi-metal 4D printing with a desktop electrochemical 3D printer, Sci. Rep. 9 (2019) 3973.
[22] M.M. Gvozdenović, B.Z. Jugović, J.S. Stevanović, T.L. Trišović, B.N. Grgur, Electrochemical polymerization of aniline, in: E. Schab-Balcerzak (Ed.), Electropolymerization, IntechOpen, 2011, pp. 77–96, Ch. 4.
[23] B. Wang, J. Tang, F. Wang, Electrochemical polymerization of aniline, Synth. Met. 18 (1987) 323–328.